H^- formation from collisional destruction of fast H_3^+ ions in noble gases

Ginette Jalbert
Departamento de Física, Pontifícia Universidade Católica do Rio de Janiero, Caixa Postal 38071, Rio de Janeiro 22453, Rio de Janeiro, Brazil

L. F. S. Coelho
Instituto de Física, Universidade Federal do Rio de Janiero, Caixa Postal 68528, Rio de Janeiro 21945, Rio de Janeiro, Brazil

N. V. de Castro Faria
Departamento de Física, Pontifícia Universidade Católica do Rio de Janiero, Caixa Postal 38071, Rio de Janeiro 22453, Rio de Janeiro, Brazil
(Received 4 February 1992)

We have studied the production of H^- by fast H_3^+ ions ($4 \leq v \leq 7$ a.u.) colliding with He, Ne, Ar, and Xe atoms. The negative-ion yields were measured as a function of target pressure and from them were extracted the H^- production cross sections, the maximum yields, and the pressure values associated with these maxima. We observed that the maximum yield is about the same for all gases and velocities in the range under consideration. This fact reveals an almost identical scaling for the H^- production, the H_3^+ destruction, and the H^- destruction cross sections. The ratio of the H^- production and the H_3^+ destruction cross sections was also verified to assume essentially the same value for all measurements. The cross sections were well fitted by a semiempirical version of the free collision model.

PACS number(s): 34.90.+q, 34.50.Lf

I. INTRODUCTION

The study of the structure and the collisional destruction of H_3^+ and similar hydrogenic ions, present in ion sources, fusion reactors, interstellar clouds, and planetary ionospheres, is important both for basic and for applied research [1–7]. Their few-body and covalent characters turn them amenable for molecular-structure calculations and allow information about their structure to be extracted from fragmentation experiments.

These ions are easily obtained from plasma ion sources. Their destruction at high velocities produces neutral and negative yields larger than the ones from H^+ projectiles. In particular, the negative yields so obtained are much larger than those from H^+ or H_2^+ projectiles, making this process useful for working with H^- beams in positive voltage accelerators [1]. Besides this practical interest of generating negative beams, this destruction process is also interesting by itself, as it is truly a three-body dissociation (at high energies electron capture, which could allow the $H_3^* \rightarrow H^- + H_2^+$ two-body channel, is a negligible process [7]).

The collisional dissociation of the H_3^+ ion has been studied mostly for some specific channels, yielding information about the H_3^+ structure. Concerning low-energy H^- production, this process has been investigated by several groups [2,3]. We should point out however, that even at this best studied energy region, cross-section data for H_3^+ destruction or H^- production are either scarce or nonexistent (see the review of H_3^+ destruction by collisions with electrons, made by Tawara *et al.* [8]). Fast H_3^+ collisions and particularly the ones leading to H^- production have received, since the pioneering work of Williams and Dunbar [4], scant attention [1,5,6].

The charge-state distributions of products from the dissociative collision of 400–800-keV H_3^+ ions (2.3–3.3 a.u.) in H_2, Ar, and air targets were measured some years ago by Nir *et al.* [5], while a more recent article by the same group [5] presented measurements at lower velocities (1.4–2.0 a.u.) for the D_3^+ fragmentation. Both works neglected channels containing negative ions, this being justified on the grounds of small negative yields.

Recently, a systematic measurement of the total H_3^+ destruction cross sections for fast H_3^+ ions colliding with He, Ne, Ar, and Xe was done in our laboratory in the 2.5–7.0-a.u. velocity range [6]. The knowledge of these cross sections is important for the present work as it allows a better modeling of the negative-ion yields as function of the target pressure.

As already mentioned, it was recently shown [1] that an appreciable amount of H^- ions may be obtained from the H_3^+ destruction. For 1200-keV H_3^+ ions colliding with Ne, Ar, and N_2, two interesting facts were also observed: the very similar behavior of the H^- and the H_3^+ destruction cross sections and the achievement of similar maximum yields for the several target gases. Together with the lack of cross-section data, these facts showed that a systematic study is needed, as a function of projectile energy and for several target gases, of the H_3^+ fragmentation leading to H^- production. We present here results for such a study, with projectile velocities ranging from 4 to 7 a.u. (1200–3700 keV) and He, Ne, Ar, and Xe

 ©1992 The American Physical Society

targets. The experimental H^- yield curves were also obtained for each target-gas–projectile-energy combination, at least up to the pressure leading to the maximum yield in each case. The negative-ion production cross-section σ_- values were extracted from the H^- and H_3^+ measured signals, in the low-pressure region, and the known σ_d^+ values [6].

These yield curves give two constants of practical interest: the maximum yield and its corresponding target pressure. Additionally, employing previous data obtained in our laboratory [6] for σ_d^+ and for σ_d^- (the sum of the single and double electron-loss cross sections [9]), it is possible to get an analytical expression for the yield curve up to and around the maximum and, subsequently, the σ_- value. However, as in the low-pressure region, the experimental growth curves were only weakly affected by the values chosen for these destruction cross sections, and as extraction of these cross sections from the yield curves presented large uncertainties, the low-pressure growth method was preferred.

Without pretending to present in this paper a theoretical analysis, if the regularities obtained in Ref. [1] were confirmed they could point to a semiquantitative interpretation, as the one presented in our previous work [6] on the destruction cross section of H_3^+. In consequence we analyzed the data in a free collision model (FCM) framework employing a semiempirical version of the FCM due to Meron and Johnson [10]. In FCM-type approaches, frequently used for the analysis of atom ionization [11] and, less commonly, for molecule excitation [12], the relevant quantity is the momentum transfer to a projectile electron and the channel will be open when this quantity exceeds a threshold. At high energies several H_3^+ destruction channels are opened and their branching ratios may be target dependent, this being associated with the polarization of the target atom, and also, in principle, velocity dependent. The fact of this not being so is an interesting question, which could be theoretically analyzed within the FCM, as done recently for atomic projectiles [13].

II. EXPERIMENTAL APPARATUS

The H^- production was measured as a function of the pressure of a differentially pumped gas target. The H_3^+ beam was obtained from the PUC/RJ4MV Van de Graaff (HVEC) accelerator, with energies in the 1.20–3.7 MeV range. A standard radio-frequency ion source was employed. Although there is an argument going on about the excited rovibrational content of H_3^+ ion beams extracted from these ion sources [14,15], in the present work, due to the high projectile kinetic energies, the cross sections are not expected to be critically dependent on this distribution. This was already verified to be so in recent measurements of the H_3^+ destruction, done at this laboratory [6].

After extraction and acceleration, the beam is momentum analyzed in a 90° magnet and collimated to a diameter of less than 0.3 mm by micrometric sliding slits. This drastic collimation reduced the beam intensity to values that were maintained always smaller than 10^3 particles per second. With these counting rates surface-barrier detectors could be employed, ensuring a continuous check of the beam energy and composition and giving the advantage of 100% efficiency. As H^- production is a largely minoritary process in respect to all other destruction channels of H_3^+ and H^- has one third of the H_3^+ energy, these checks are not only necessary but also feasible.

The gas target cell and the pressure measurement employing a thermocouple device were already described [6,9]. In brief, it is a cell 10 cm long coupled to a two-axis goniometer, for easy alignment, with entrance and exit apertures of 0.8 and 2.0 mm, respectively, and placed in a large chamber evacuated by a 200-l/s diffusion pump. Entrance and exit vacuum impedances isolate this large chamber from the remaining beam line. The vacuum outside the chamber is further maintained by two diffusion pumps, each one installed nearby one impedance. With this arrangement a pressure gradient of nearly a factor of 10^3 was obtained between the gas cell and the surrounding vacuum and this, even considering that the target detector distance as 15 times larger than the cell length, led to a very small influence of the residual pressure on the beam line due to the gas used on the cell.

However, due to the very small H^- production cross sections for the lighter targets, these data were more affected by heavy element impurities, including air and water being desorbed by the pipe which brought the gas to the cell and residual gases from background and from previous experimental runs. Several cautions were taken to avoid this problem including a cooling system in which the He and Ne gases leaving the bottles traverse a liquid-nitrogen trap before entering the cell. As we will later see, the results for He were particularly good when compared with the present results for the other gases and with the older He results [6], obtained in our laboratory without such a trap, although similar comparisons made for Ne show that the present results have relatively larger fluctuations. The gas target thickness uncertainty arising from the calibration of the thermocouple against a McLeod gauge was estimated as 10%, being due both to the calibration procedure and the McLeod gauge uncertainty itself. The target gases nominal purities were 99.99%.

After the gas cell there is another magnet, with exists at the angles of 0°, ±15°, ±30°, and ±45° (one in the beam line direction and three on each side). The simultaneous measurement of H^- at −45° and H_3^+ at +15° allows the yield to be obtained. The H^- ions were detected by a large (25-mm-diam) surface-barrier detector and another detector, with a diameter ~15 mm, was employed for the H_3^+ ions. Both detectors are placed at 1.5 m from the gas target. In each run the H^- beam was centered by varying the switch magnet current and, afterwards, the H_3^+ beam was centered by moving its detector in two directions on the plane normal to this deflected beam. Even with this procedure, the maximum diameter of the H^- beam at the detector position must be smaller than the detector size to ensure full collection. For 2700-keV H_3^+ ions the measured value [16] of this maximum diam-

eter is 5 mm and as it scales to the inverse of the projectile velocity, even for the least favorable case of 1200-keV H_3^+ ions, it will be less than 8 mm.

To avoid pileup problems the counting rate of the H_3^+ detector was less than 10^3 counts per second, as already stated. The H^- and the H_3^+ pulses were counted in two scalers, and during the experiment there was an all-time monitoring by oscilloscopes. Starting and stopping of the counting in each detector were respectively made by opening and closing a beam stopper.

III. DATA ANALYSIS AND RESULTS

In order to extract cross sections from the numbers of detected H^- and H_3^+ transmitted ions, we need a model accounting for (a) the direct H^- production from H_3^+, (b) the molecular ion destruction by any process, and (c) multiple collision processes either creating or destroying negative ions. The production of H followed by an electron capture to H^-, the production of H_2 followed by its breakup into $H^- + H^+$, and the H^- destruction are three examples of these higher-order processes (c).

As was shown in Ref. [1], the maximum for the H^- production from H_3^+ is higher than for incident H and takes place at about the same target thicknesses. This is an evidence that the main process is the direct H^- production from H_3^+, affected by the previous destruction of molecular ions and by the posterior destruction of negative ions. In this approximation the equation system describing low-pressure H^- production is

$$\frac{dN_+}{dx} = -N_+ \sigma_d^+ n \ , \qquad \frac{dN_-}{dx} = (N_+ \sigma_- - N_- \sigma_d^-) n \ , \tag{1}$$

where N_+ and N_- are, respectively, the H_3^+ and the H^- particle flows inside the target as a function of the position x, n is the target density, σ_- is the H^- production cross section, σ_d^+ is the H_3^+ destruction cross section, and σ_d^- is the sum of the single and the double electron-loss cross sections for an H^- ion.

Solving the above system one gets the numbers of detected H_3^+ and H^- ions, respectively, N_+ and N_-:

$$N_+(\pi) = N_+(0) e^{-\sigma_d^+ \pi} \ , \tag{2a}$$

$$N_-(\pi) = N_+(0) \sigma_- \left[\frac{e^{-\sigma_d^+ \pi} - e^{-\sigma_d^- \pi}}{\sigma_d^- - \sigma_d^+} \right] , \tag{2b}$$

where π is the target thickness (the product of the target length l to its density n), $N_+(0)$ is the number of molecular ions incident on the cell, and the background gas contribution has been neglected. The theoretical expression for the H^- yield F, defined as $N_-(\pi)$ divided by the $N_+(0)$, is, in this case,

$$F_{\text{theor}} = \sigma_- \left[\frac{e^{-\sigma_d^+ \pi} - e^{-\sigma_d^- \pi}}{\sigma_d^- - \sigma_d^+} \right] , \tag{3}$$

requiring the knowledge of the two destruction cross sections. The employed values came from Refs. [6] and [9], except for σ_d^- in Xe, after an interpolation procedure that minimized the propagation of their fluctuations. For H_3^+ the excellent fit $1/\sigma_d^+ = a + bv^2$ was used [6], coming from a semiempirical version of the free collision model [10] (additional comments in Sec. IV). For H^- we used a polynomial v^{-a}, with $1 < a < 2$, as already discussed in Ref. [9].

The experimental results cannot be immediately compared to the above theoretical yield F. We first have to obtain the number of incident projectiles $N_+(0) = N_+(\pi) e^{\sigma_d^+ \pi}$ accounting for H_3^+ attenuation in the target gas (H_3^+ attenuation in the residual gas was neglected). We must then consider H^- production and destruction in the residual gas, present even at zero target pressure. With these approximations the experimental yield becomes

$$F_{\text{expt}} = \frac{N_-(\pi)}{N_+(\pi) e^{\sigma_d^+ \pi}} \ , \tag{4a}$$

to be theoretically described by

$$F_{\text{theor}} = (\sigma_- \pi + B) \left[\frac{e^{-\sigma_d^+ \pi} - e^{-\sigma_d^- \pi}}{(\sigma_d^- - \sigma_d^+)\pi} \right] \sim \sigma_- \pi \left[\frac{e^{-\sigma_d^+ \pi} - e^{-\sigma_d^- \pi}}{(\sigma_d^- - \sigma_d^+)\pi} \right] + B \ , \tag{4b}$$

where B was taken as the ratio between the measured H^- and H_3^+ ions at the residual pressure.

In the lower part of Fig. 1 a comparison is presented

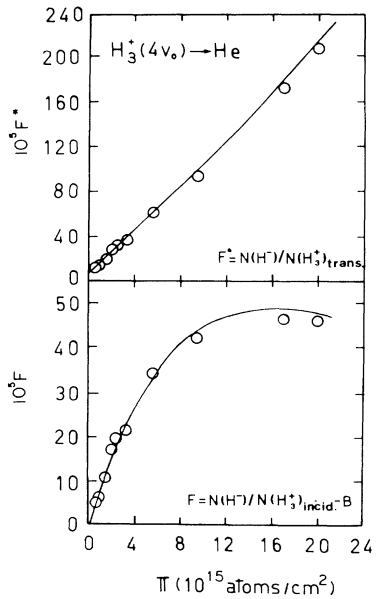

FIG. 1. Typical experimental results for the yield as function of the target thickness. The upper part shows the ratio F^* of the numbers of transmitted H^- and H_3^+ ions and the lower shows the ratio F of the number of transmitted H^- to the incident H_3^+ ions. In both cases they are multiplied by 10^5.

between typical experimental (open circles), after subtracting the constant B, and theoretical (full line) curves F. For low target thicknesses we get essentially a straight line, corresponding to the expansion of expression (4b) $F \sim \sigma_- \pi$. Systematic variation of σ_d^- up to a factor of 2 showed that the fit quality suffered a very small influence and the χ^2 estimated value varied by less than 5%.

In the upper part of Fig. 1 we present in a different way the same basic data of the lower part. The data are now shown as they were obtained from the scaler readings, i.e., with $F^*_{\text{expt}} = N_-(\pi)/N_+(\pi)$ being indicated as open circles. This figure illustrates a typical background value and shows the validity of the linear approximation. In order to be consistent with our previous normalization, given in Eqs. (3) and (4), the experimental F^* values have to be compared to

$$F^*_{\text{theor}} = \sigma_- \pi \left[\frac{1-e^{-\alpha\pi}}{\alpha\pi} \right] + B e^{\sigma_d^+ \pi} , \tag{5}$$

where α is the $\sigma_d^- - \sigma_d^+$ difference. At low target densities we again obtain a straight line $F^*_{\text{theor}} \sim \sigma_- \pi + B$. This straight line reproduces well the data up to relatively large pressures, not far from the maximum.

Although the fit of the low-pressure data suffers little influence from the chosen value for α and probably even less from the multiple collision processes leading to H^- production, this could not be the case near the maximum yield. In fact Rosner and co-workers [5] have shown that H^0 production could be a very important channel for H_3^+ destruction. To see the importance of the two-step H^- formation when first a hydrogen atom is originated in the H_3^+ breakup and then this atom captures one electron, the equation system,

$$\frac{dN_+}{dx} = -N_+ \sigma_d^+ n , \tag{6a}$$

$$\frac{dN_-}{dx} = (N_+ \sigma_- + N_0 \sigma_{01} - N_- \sigma_d^-) n , \tag{6b}$$

$$\frac{dN_0}{dx} = (N_+ \sigma_0 - N_0 \sigma_d^0) n , \tag{6c}$$

TABLE I. (a) Pressures, given in 10^{-3} Torr, leading to maximum H^- yields at different projectile velocities and for different target gases. (b) Maximum H^- yields F (10^{-4}), corresponding to the pressure values of (a).

Element \ Velocity (a.u.)	4	5	6	7
	(a)			
He	48	61	77	96
Ne	12	14	18	22
Ar	5.8	7.2	8.8	10
Xe	2.8	3.2	3.7	4.4
	(b)			
He	4.6	4.3	4.0	4.0
Ne	4.0	3.5	3.6	4.2
Ar	4.2	4.4	4.2	4.5
Xe	2.3	2.4	2.4	2.4

TABLE II. H^- production cross section σ_- (10^{-19} cm^2) for different velocities and target gases.

Element \ Velocity (a.u.)	4	5	6	7
He	0.84	0.63	0.46	0.33
Ne	2.86	1.85	1.67	1.58
Ar	6.06	5.39	4.12	3.72
Xe	7.23	6.24	5.50	4.72

must be solved, where N_0 is the H flow inside the target as a function of the position x, σ_0 is the H production cross section, and σ_d^0 is the sum of the capture $\sigma_{0\bar{1}}$ and the loss σ_{01} cross sections. We get for the yield F_{theor},

$$F_{\text{theor}} = \frac{N_-(\pi)}{N_+(0)} = e^{-\sigma_d^+ \pi} \left[\left[\sigma_- + \frac{\sigma_0 \sigma_{0\bar{1}}}{\beta} \right] \left[\frac{1-e^{-\alpha\pi}}{\alpha} \right] + \frac{\sigma_0 \sigma_{0\bar{1}}}{\beta} \left[\frac{e^{-\beta\pi} - e^{-\alpha\pi}}{\beta - \alpha} \right] \right] , \tag{7}$$

with β being the difference $\sigma_d^0 - \sigma_d^+$.

The second term of expression (7) may account for the 10% difference, in the worst case, between the measured and the calculated maximum yields. This was verified by fitting the data to this more general expression. As the χ^2 surface is very flat relatively to variations of the $\sigma_0 \sigma_{0\bar{1}}/\beta$ constant, these fits cannot lead to precise values for σ_0, $\sigma_{0\bar{1}}$, or β.

The position and the magnitude of the maximum H^- yields are presented in Table I. An average uncertainty of ±15% must be assigned to the maximum yield while the flatness of the yield near the maximum led to a larger estimated (±20%) error for the position.

Not only our experimental values agree well with the ones expected from previously measured σ_d^+ and σ_d^- cross sections, when these are available, but it should also be pointed out that large magnitudes for the maximum yield were obtained. From the practical point of view, a user of Table I information may choose a pressure value and a gas target in order to have a good yield with the minimum gas consumption and the least expensive gas.

The experimental cross sections for H^- formation from H_3^+ are presented in Table II. The values of Ref. [1], smaller than our values by about 20%, were obtained from the maximum yields and not from growth curves. These yields are, as already discussed, dependent on α and on second-order processes and this may explain this discrepancy.

IV. DISCUSSION AND CONCLUSIONS

One striking feature of Table I(b) is the velocity independence of the maximum yield for all four gases. This

suggests the proportionality of the three most relevant cross sections for H^- production, namely σ_-, σ_d^-, and σ_d^+.

A second characteristic of the maximum yield data is to present an almost constant value for the three smaller targets—He, Ne, and Ar—of 4.1×10^{-4}, with a standard deviation of 0.5 (12%). The Xe data show a 40% smaller value but the same velocity-independent behavior still remains.

These facts point to the existence of "universal" noble gas scaling laws for the several excitation processes of H_3^+ and H^- ions. Although the velocity range is not too wide, any tentative explanation for these scaling laws should consider the largely different numbers of target electrons, going from 2 in helium to 54 in xenon, and the variety of processes. In a simple model, the minimum exchanged momentum is the relevant quantity to describe any of these three processes (H^- production and destruction and H_3^+ destruction). As this momentum is of the same order of magnitude needed to either excite or remove the outer electrons, the probability for any of these three processes to occur is the one for outer target electron excitations times a constant of near-unity value. Particularly for electron-impact ionization of noble gases, the cross sections scale very well with the square of the Hartree-Fock radius of the outer electrons [17]. For these outer electrons both the average orbital radius and the ionization potentials are well described by simple power laws of the atomic number Z.

In the present case we are dealing with outer electron excitation both to continuum and discrete states. This excitation process may be illustrated by the simplified FCM version of Ref. [10], where the target is considered a pointlike scattering center and the contribution of its electrons to the cross section is given by a form factor. In the Xe case, however, the similar target and projectile sizes make it harder to describe the processes as *free* projectile electrons interacting with the noble gas outer electrons as it is very likely for the projectile to come inside the target outer shell.

This analysis is reinforced when one looks to the branching ratio data, presented in Table III, for H^- production in relation to H_3^+ destruction. It is again striking that all branching ratios, independent of velocity or target gas, are constant (the values oscillate within 15% of the average 1.27×10^{-3}).

TABLE III. Ratio of the H^- production cross section σ_- for the H_3^+ destruction cross section σ_d^+. (This ratio, given in units of 10^{-3}, gives the probability for an H^- ion to arise from the H_3^+ destruction.)

Element \ Velocity (a.u.)	4	5	6	7
He	1.15	1.28	1.31	0.97
Ne	1.31	1.03	1.11	1.44
Ar	1.40	1.53	1.36	1.65
Xe	1.21	1.21	1.16	1.25

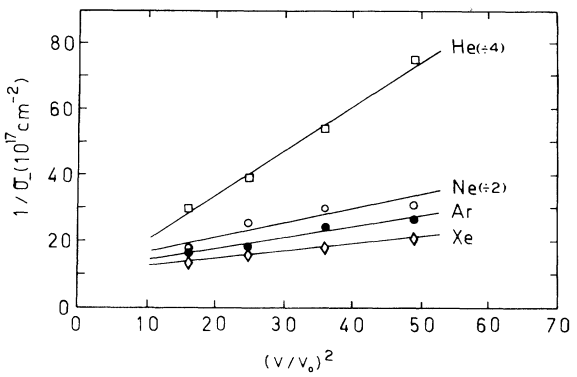

FIG. 2. Experimental H^- production cross sections for the several targets and projectile velocities. The results are plotted as σ_-^{-1} vs v^2 and being fitted to straight lines, justified on a semiempirical basis. The velocities are in atomic units and the inverse of the cross sections in 10^{17} cm^{-2}.

Finally Fig. 2 shows the σ_- cross sections for the several targets, with plots of $1/\sigma_-$ against v^2, similar to Ref. [6]. As indicated by the semiempirical version of the free collision model due to Meron and Johnson [10], this gives a straight line $1/\sigma_- = A + Bv^2$, where A and B are constants accounting for the target excitation and also depending on an average orbital radius for the target electrons.

Recent calculations done by Riesselman, Anderson, and Durand [13], based on an improved semiclassical FCM, seem to corroborate our analysis. They used the free collision model to calculate single electron-loss cross sections for H(1s). With an improved version of the geometrical analysis of Dewagan and Walters [11] they also calculated double electron-loss cross sections for incident H and H^- projectiles. The results are in excellent agreement with existing data, including a work done in this laboratory with these projectiles [9].

Considering valid the Salpeter [12] approach of treating molecular excitation to a self-dissociating state as similar to atomic ionization, and this seems to be substantiated by previous [6] and present experimental results, an extension of the procedure detailed in Ref. [13] to our two-electron molecular case is, in principle, possible. This extension will present, however, a few particular problems due to some simplifying geometrical assumptions no longer valid, and also due to the insufficient knowledge of distributions for (a) the H_3^+ electron velocity in the projectile frame and (b) the dissociation energy. Although we did not make this extension, the fact that the FCM, either in complete [11,13] or in semiempirical [10] versions, describes well a variety of processes, with several projectiles and targets and in a wide energy range, added to the fact of our previous [6] and present results being well described by the semiempirical version [10], could be a motivation for future work in the FCM description of molecular collisions and also for more refined calculations.

ACKNOWLEDGMENTS

L.F.S.C. gratefully acknowledges the hospitality of researchers and staff members of the Van de Graaf accelerator of Pontifícia Universidade Católica at Rio de Janeiro. This work was supported in part by the Financiadora de Estudos e Projectos, Conselho Nacional de Desenvolvimento Científico e Technológico and Fundação de Apoio à Pesquisa do Estado do Rio de Janeiro.

[1] N. V. de Castro Faria, M. J. Gaillard, J. C. Poizat, and J. Remillieux, Nucl. Instrum. Methods Phys. Res. B **43**, 1 (1989).

[2] D. L. Montgomery and D. H. Jaecks, Phys. Rev. Lett. **51**, 1862 (1983); D. H. Jaecks, O. Yenen, C. Engelhardt, and L. Wiese, Nucl. Instrum. Methods Phys. Res. B **40/41**, 225 (1989); O. Yenen, D. H. Jaecks, and L. M. Wiese, Phys. Rev. A **39**, 1767 (1989).

[3] I. Alvarez, H. Martinez, C. Cisneros, A. Morales, and J. de Urquijo, Nucl. Instrum. Methods Phys. Res. B **40/41**, 245 (1989); I. Alvarez, C. Cisneros, J. de Urquijo, and T. J. Morgan, Phys. Rev. Lett. **53**, 740 (1984).

[4] G. W. McClure, Phys. Rev. **130**, 1852 (1963); J. F. Williams and D. N. F. Dunbar, *ibid.* **149**, 62 (1966); K. H. Berkner, T. J. Morgan, R. V. Pyle, and J. W. Stearns, Phys. Rev. A **8**, 2870 (1973).

[5] D. Nir, B. Rosner, A. Mann, and J. Kantor, Phys. Rev. A **18**, 156 (1978); S. Abraham, D. Nir, and B. Rosner, *ibid.* **29**, 3122 (1984).

[6] W. Wolff, L. F. S. Coelho, H. E. Wolf, and N. V. de Castro Faria, Phys. Rev. A **45**, 2978 (1992).

[7] M. J. Gaillard, A. G. de Pinho, J. C. Poizat, J. Remillieux, and R. Saoudi, Phys. Rev. A **28**, 1267 (1983).

[8] H. Tawara, Y. Itikawa, H. Nishimura, and M. Yoshino, J. Phys. Chem. Ref. Data **19**, 617 (1990).

[9] D. P. Almeida, N. V. de Castro Faria, F. L. Freire, Jr., E. C. Montenegro, and A. G. de Pinho, Phys. Rev. A **36**, 16 (1987).

[10] M. Meron and B. M. Johnson, Phys. Rev. A **41**, 1365 (1990).

[11] D. P. Dewagan and H. R. J. Walters, J. Phys. B **11**, 3983 (1978).

[12] E. E. Salpeter, Proc. Phys. Soc. London Sect. A **63**, 1297 (1950).

[13] R. Riesselman, L. W. Anderson, and L. Durand, Phys. Rev. A **43**, 5934 (1991).

[14] B. Peart and K. T. Dolder, J. Phys. B **7**, 1567 (1974); D. L. Smith and J. H. Futrell, *ibid.* **8**, 803 (1975); V. G. Anicich and J. H. Futrell, Int. J. Mass Spectrom. Ion Processes **55**, 189 (1983/1984).

[15] H. Hus, F. Youssif, A. Sen, and J. B. A. Mitchell, Phys. Rev. A **38**, 658 (1988).

[16] N. V. de Castro Faria, W. Wolff, L. F.S. Coelho, and H. E. Wolf, Phys. Rev. A **45**, 2957 (1992).

[17] H. Deutsch and T. D. Mark, Int. J. Mass. Spectrom. Ion Processes **79**, R1 (1987).